NUMERICAL SIMULATION OF THE NON-AXISYMMETRIC MAGNETOROTATIONAL INSTABILITY IN A DOMINANTLY AZIMUTHAL MAGNETIC FIELD

GALINDO, Vladimir, STEFANI, Frank and SEILMAYER, Martin
Helmholtz-Zentrum Dresden-Rossendorf
P.O. Box 510119, D-01314 Dresden, Germany
email: v.galindo@hzdr.de

Abstract: In a Taylor-Couette experiment on the non-axisymmetric version of the magnetorotational instability, performed by Seilmayer et al. [1], a dominantly azimuthal magnetic field was created by a central vertical copper rod connected to the power source by two horizontal rods at a height of approximately 0.8 m below and above the cylindrical volume. The liquid metal flow in the cylindrical gap between the cylinders was simulated using the OpenFoam library including a Poisson equation for the determination of the induced electric potential. The slight deviation from a purely axisymmetric azimuthal imposed magnetic field turns out to have a surprisingly strong effect on both the critical Hartmann number and the flow structure of the instability.

1. Introduction

Rotating flows with a radially increasing angular momentum are hydrodynamically stable but can be destabilized by magnetic fields via the magnetorotational instability (MRI) [2, 3]. If the magnetic field is purely azimuthal, we obtain a non-axisymmetric version of MRI [4, 5], called the azimuthal magnetorotational instability (AMRI), which plays a central role in the concept of the MRI dynamo in accretion disks [6].

In a recent liquid metal experiment [1], AMRI was shown to set in approximately at the predicted value of the magnetic field strength. Yet, there were some significant differences between the observed and numerically predicted rms values of the velocity. In this paper, these discrepancies are explained by the strong sensitivity of the AMRI with respect to slight deviations of the applied magnetic field from axisymmetry. For this purpose, we simulate the experiment using the OpenFoam library including a Poisson equation for the determination of the induced electric potential.

2. Problem formulation

Figure 1 shows a sketch of the considered problem which comprises the main features of the magnetized Taylor-Couette experiment as reported by Seilmayer et al. [1]. A strong axial electric current I_a flows in a vertical copper rod creating in the melt a dominantly azimuthal magnetic field.

Due to the contributions of the connections to the power supply, the applied magnetic field is not anymore purely azimuthal and axisymmetric, but has also radial and axial components (see Fig 2). In the case of an axisymmetric azimuthal magnetic field we would have $\boldsymbol{B} = B\ \boldsymbol{e}_\varphi$ with a maximal value at the inner cylinder $B_{max} = B(R_i) = \mu_0 I_a/(2\pi R_i) \approx 80\ mT$ (for $I_a = 16\ kA$). Whereas the axial component B_z is three orders of magnitude smaller than the azimuthal component B_φ, the B_r component can not be neglected and should be taken into account.

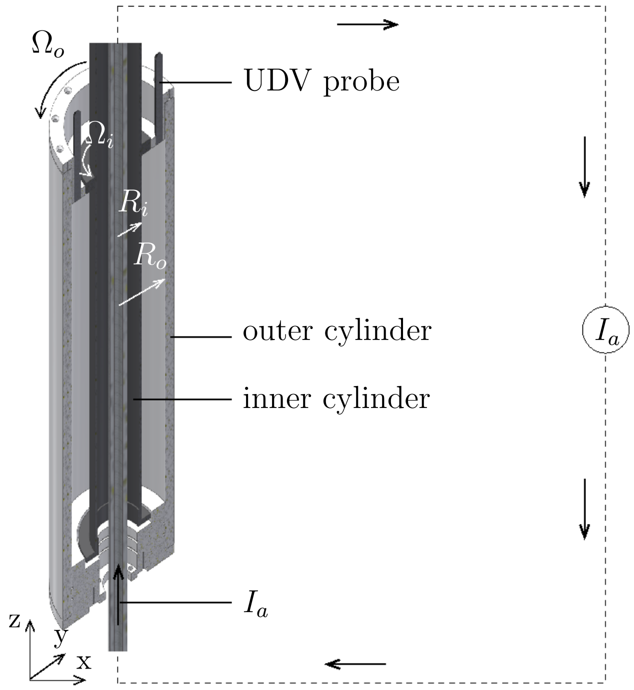

Figure 1: Sketch of the geometry of the experiment.

2.1. Governing equations

The interaction between the induced electric current density $\boldsymbol{j}$ and the magnetic field $\boldsymbol{B}$ yields the induced electromagnetic force density $\boldsymbol{j} \times \boldsymbol{B}$ (Lorentz-force) in the melt. Using the radius of the inner cylinder R_i as the length scale, the azimuthal velocity of the inner cylinder $\Omega_i R_i$ as the velocity scale, defining $B_i = B(R_i)$, taking into account Ohm's law $\boldsymbol{j} = \sigma(-\nabla\Phi + \boldsymbol{u} \times \boldsymbol{B})$ and the electric charge conservation $\nabla \cdot \boldsymbol{j} = 0$, we obtain the dimensionless equation for the momentum conservation

$$\dot{\boldsymbol{u}} + (\boldsymbol{u} \cdot \nabla)\boldsymbol{u} = -\nabla p + \frac{1}{Re}\Delta \boldsymbol{u} + \frac{Ha^2}{Re}\big(-\nabla\Phi + \boldsymbol{u} \times \boldsymbol{B}) \times \boldsymbol{B}\,. \tag{1}$$

Here we use the definitions $Re = \Omega_i R_i^2/\nu$ and $Ha = \sqrt{\dfrac{\sigma}{\rho\,\nu}} B_i R_i$ for the Reynolds and Hartmann numbers, respectively. The electric potential Φ can be determined by the Poisson equation:

$$\Delta\Phi = \nabla \cdot (\boldsymbol{u} \times \boldsymbol{B})\,. \tag{2}$$

We solve equations (1) and (2) simultaneously in the low induction approximation, i.e. the magnetic induction B is considered to be independent of the flow velocity and is computed only once using the Biot-Savart law. For more details about the numerical method see [7].

We use no-slip boundary conditions for the velocity at the rigid walls, and slip boundary conditions at the narrow open slits between the outer and inner end-caps. At the external wall, i.e. the outer copper cylinder, we chose for the electric potential $\Phi = 0$, and for the rest of the boundaries we apply insulating boundary conditions ($j_n = 0$).

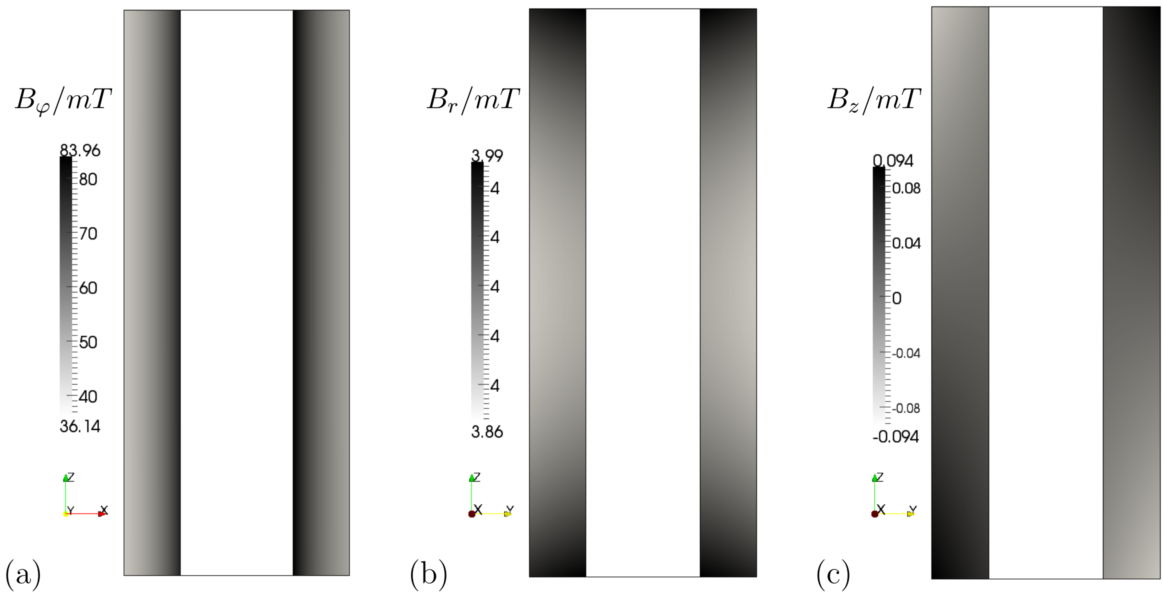

Figure 2: Magnetic field components B_φ (a) in the "xz"-plane parallel to the current loop, and B_r (b) and B_z (c) in the "yz" plane.

3. Results

Figure 3 shows the numerically obtained drift frequency of the AMRI mode with $m = 1$ for the particular case $Re = 1480$ and $\mu = \Omega_o/\Omega_i = 0.26$, in comparison with the 1-d linear stability analysis for an infinitely long cylinder [5] and with the experimental results from [1].

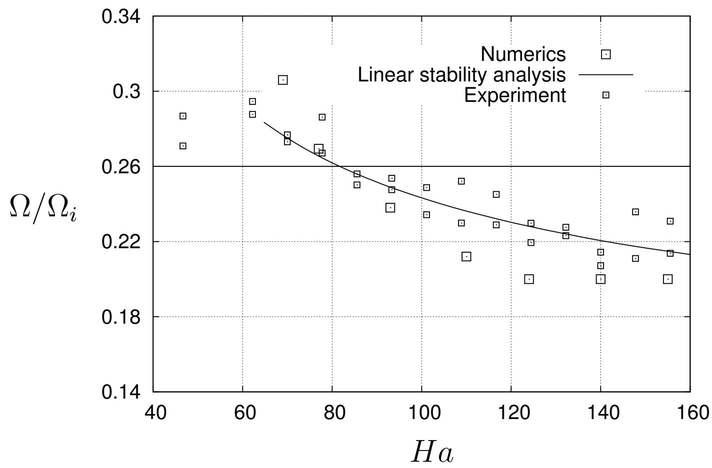

Figure 3: Drift frequency of the azimuthal mode $m = 1$ for $Re = 1480$ and $\mu = \Omega_o/\Omega_i = 0.26$.

Figure 4 shows the computed velocity profiles $u_z(r = 0.07\ m, z)$ of the azimuthal mode $m = 1$ as a function of time for different values of the rotation ratio $\mu = \Omega_o/\Omega_i$ in the hypothetical case of a purely axisymmetric azimuthal magnetic field. Evidently, the AMRI disappears with increasing μ.

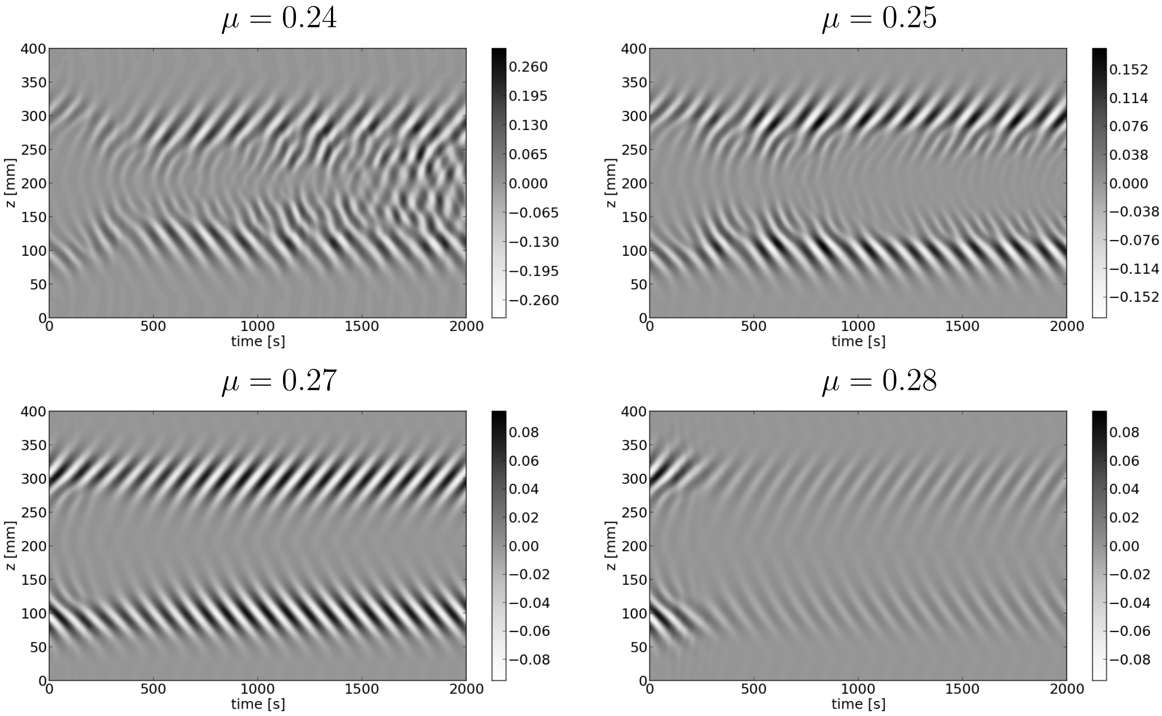

Figure 4: Velocity profiles $u_z(r = 0.07\ m, z)$ of the azimuthal mode $m = 1$ over time for different values of the rotation ratio $\mu = \Omega_o/\Omega_i$ for the case of an axisymmetric imposed azimuthal magnetic field.

Figure 5 shows the isosurface of the axial velocity component u_z for the case of axisymmetric (left) and non-axisymmetric applied magnetic field (right). For axisymmetry, the resulting pattern represents a spiral, rotating slightly slower than the outer cylinder. This spiral is concentrated approximately in the middle of the upper and lower halves of the cylinder, where we observe a preference for either the upward moving or the downward moving spiral. Since such a symmetry breaking would not appear in an infinite length system, it must be attributed to the (minor) flow modifications due to the end walls. The corresponding simulation for the case that the deviation of the applied magnetic field from axisymmetry is correctly taken into account is shown on the r.h.s. of Figure 5. The effect is remarkable: the formerly clearly separated spiral structures now also fill the middle part of the cylinder and penetrate into the other halves. It is interesting to note that a similar picture of interpenetrating spirals had been observed in simulations of a corotating spiral Poiseuille flow [8].

4. Conclusions

We have shown that a careful 3-d simulation is needed to understand the experimental results of a recent experiment on AMRI. The observed, and numerically confirmed, strong sensitivity of AMRI with respect to a slight symmetry breaking deserves further attention. Present work is devoted to the question whether the AMRI shifts also to higher values of the rotation ratio of outer to inner cylinder when the symmetry breaking of the applied field is taken into account. It would be of significant astrophysical importance if slight modifications of an azimuthal field would allow the inductionless AMRI to apply also to rotation profiles as shallow as the Keplerian one.

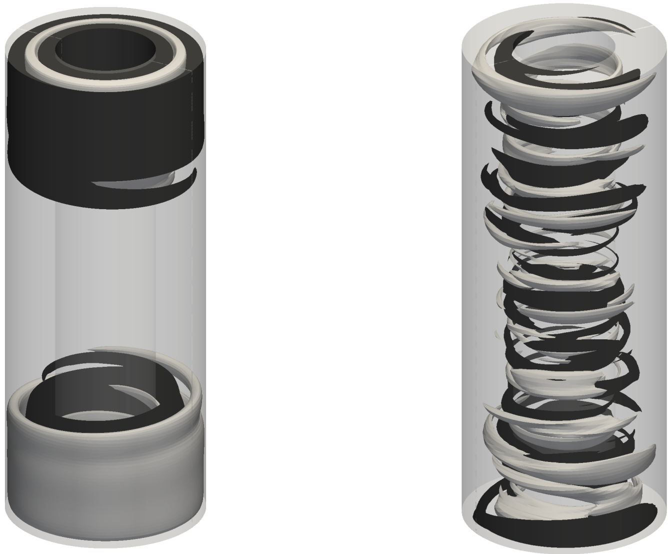

Figure 5: Isosurface of the axial velocity component u_z for the cases axisymmetric (left) and non-axisymmetric (right) applied magnetic field ($Ha = 124$) showing different flow structures.

5. Acknowledgment

We acknowledge support from Deutsche Forschungsgemeinschaft under Grant No. STE 991/1-2, and from the Helmholtz Alliance LIMTECH.

References

[1] Seilmayer, M. et al.: Phys. Rev. Lett., submitted (2013); arXiv:1311.7223

[2] Velikhov, E. P.: Sov. Phys. JETP 36 (1959) 995

[3] Balbus, S. A.; Hawley, J.F.: Astrophys. J. 376 (1991) 214

[4] Hollerbach, R. et al.: Phys. Rev. Lett. 104 (2010) 044502

[5] Rüdiger, G. et al.: Mon. Not. R. Astr. Soc. 438 (2014) 271

[6] Herault, J. et al.: Phys. Rev. E 84 (2011) 036321

[7] Weber, N. et al.: New J. Phys. 15 043034 (2013) 043034

[8] Avila, M. et al.: Phys. Fluids 18 043034 (2006) 064101